Advances in Applied Mathematics and Mechanics
Adv. Appl. Math. Mech., Vol. 7, No. 4, pp. 496-509

DOI: 10.4208/aamm.2014.m611
August 2015

Meshless Collocation Method for Inverse Source Identification Problems

Fuzhang Wang[1,*] and Zhaoxing Ma[2]

[1] *College of Mathematics, Huaibei Normal University, Huaibei 235000, China*
[2] *School of Electrical Engineering and Automation, Jiangsu Normal University, Xuzhou 221116, China*

Received 8 May 2014; Accepted (in revised version) 28 October 2014

Abstract. A novel meshless scheme is proposed for inverse source identification problems of Helmholtz-type equations. It is formulated by the non-singular general solutions of the Helmholtz-type equations augmented with radial basis functions. Under this meshless scheme, we can determine smooth source terms from partially accessible boundary measurements with accurate results. Numerical examples are presented to verify validity and accuracy of the present scheme. It is demonstrated that the present scheme is simple, accurate, stable and computationally efficient for inverse smooth source identification problems.

AMS subject classifications: 65M10, 78A48

Key words: Meshless method, Helmholtz equation, source function.

1 Introduction

Inverse source problems are very important in many branches of science and engineering. They have attracted great attentions from many researchers because of their applications to many practical examples. Many theoretical and numerical studies have been executed over recent years. For an overview of this branch, we refer readers to references [8,14,21, 23,25] and references therein.

Most of the previous numerical works are focused on the boundary element method [10]. Ohnaka and Uosaki [27] developed a boundary element approach for identifying the external force applied to a number of points on the domain of a distributed parameter system. By using DRM, Kagawa et al. [19] considered the identification of unknown electric charge distribution. Trlep et al. [31] presented the use of the dual

*Corresponding author.
Email: wangfuzhang1984@163.com (F. Z. Wang), 82563433@qq.com (Z. X. Ma)

 ©2015 Global Science Press

https://doi.org/10.4208/aamm.2014.m611 Published online by Cambridge University Press

reciprocity boundary element method (DRM) for the solution of the inverse problem described with Poisson's equation. The boundary element method is also used to compute the unknown surface velocity distribution on a complex acoustic source from measured acoustic field data [30]. The use of the inverse boundary element method (BEM) to identify aeroacoustic noise sources is explored in [24].

One of the boundary-type meshless method, the method of fundamental solutions [9, 15, 22], is shown to be superior to the boundary element method. It is becoming very popular for solving both direct and inverse problems [1, 6, 29]. By using the method of fundamental solutions, Jin and Marin considered the inverse source potential problem $\nabla^2 u(\mathbf{x})=f(\mathbf{x})$ associated with the steady-state heat conduction with the extra assumption that $\Delta f=0$ [18]. Their main idea is to, by the fact that f is harmonic, transform the original problem into a fourth-order partial differential equation. The resulting partial differential equation can be solved using numerical methods. Recently, Wang and his coworkers [35] considered a generalized case in a sense that the unknown source f need not be harmonic.

Note that most previous literatures are focused on the indirect approaches, i.e., the dual reciprocity method is used during the solution process. In this paper, a direct meshless collocation formulation is proposed for inverse smooth source problems associated with Helmholtz-type equations. The fictitious boundary used in [35] is eliminated in the current proposed method. Our problem is, first to give the meshless collocation formulation, then to study the effect of related parameters and stability issue from partially accessary boundary data.

The outline of this paper is as follows. In Section 2, we briefly state the inverse source problems. Section 3 established the meshless collocation formulation in terms of nonsingular general solutions of the Helmholtz-type equations augmented with radial basis functions. To deal with the ill-conditioned interpolation matrix system, we employ the Tikhonov regularization (TR) method under parameter choice of generalized cross validation. Numerical examples are discussed for both circular and irregular domains in Section 4. Section 5 concludes this paper with some additional remarks.

2 Problem description

Most acoustic sources encountered in real applications always have definite characters whcih can be modeled to the following Helmholtz governing equation

$$\nabla^2 u(\mathbf{x})+k^2 u(\mathbf{x})=f(\mathbf{x}), \quad \mathbf{x}\in\Omega, \tag{2.1}$$

under boundary conditions $u(\mathbf{x})=\bar{u}(\mathbf{x})$ on Dirichlet boundary Γ_D and $q(\mathbf{x})=\bar{q}(\mathbf{x})$ on Neumann boundary Γ_N, where $\bar{u}(\mathbf{x})$ and $\bar{q}(\mathbf{x})$ are pre-defined functions. $u=u(\mathbf{x})$ is the unknown field function, Ω is the physical domain with physical boundary $\partial\Omega$ $(=\Gamma_D\cup\Gamma_N)$, k and n are wavenumber and unit normal vector, respectively. In cases that the boundary is only partially accessible, the known functions $\bar{u}(\mathbf{x})$ and $\bar{q}(\mathbf{x})$ are given boundary conditions on $\Gamma\subset\partial\Omega$ simultaneously to ensure that the boundary value problems are solvable. We aim to determine the unknown source function $f=f(\mathbf{x})$ under the circumstances.

https://doi.org/10.4208/aamm.2014.m611 Published online by Cambridge University Press

For homogeneous problems, i.e., $f(\mathbf{x})=0$ in Eq. (2.1), the theory of many meshless methods lies in that the approximate solution $u_N(\mathbf{x})$ can be expressed in terms of radial basis functions $Q(\cdot)$

$$u_N(\mathbf{x})=\sum_{j=1}^{N}c_jQ(\mathbf{x},\mathbf{y}_j), \tag{2.2}$$

where $\mathbf{y}_j$ are source points on the physical domain/boundary, c_j are coefficient to be determined, N the total number of source points.

For nonhomogeneous problems, i.e., $f(\mathbf{x})\neq 0$ in Eq. (2.1), some indirect techniques like the dual reciprocity method and the multiple reciprocity method are introduced to deal with the nonhomogeneous terms for direct problems [3,28,32,38]. Our purpose is to recover the unknown source terms $f(\mathbf{x})$ by using the boundary data under a direct way. The main procedure of the proposed method is described in the following section.

3 Direct methodology for inverse problems

3.1 Meshless collocation formulation

Motivated by the theory of Eq. (2.2), we propose to couple the non-singular general solutions of the Helmholtz-type equations augmented with radial basis functions to solve Eq. (2.1) with an unknown general source function f. More specifically, the approximate solution $u_N(\mathbf{x})$ of Eq. (2.1) can be expressed as

$$u(\mathbf{x})=\sum_{l=1}^{N}\alpha_l\varphi_l(\mathbf{x},\mathbf{x}_l)+\sum_{m=1}^{N_B}\beta_mG(\mathbf{x},\mathbf{x}_m), \tag{3.1}$$

where $N=N_B+N_I$, N_B and N_I are the numbers of total boundary and internal points, respectively. The internal points are considered for the reason that the solution accuracy for nonhomogeneous problems also relates to the number of the internal points. $G(\mathbf{x},\mathbf{y})=J_0(kr)$ is the non-singular general solutions for the Helmholtz equation with J denoting the Bessel function of the first kind and $r=\|\mathbf{x}-\mathbf{y}\|$ the Euclidean distance [4,5,40]. The basis $\{\varphi_l\}_{l=1}^{N}$ is a set of user-chosen approximate-basis-functions. In this paper, we choose the excellent MQ $\psi_l=\sqrt{r_l^2+c^2}$ as the radial basis function [20].

In order to determine the unknowns α_l and β_m, collocating the numerical expansion (3.1) at N_I internal points and enforcing boundary conditions at N_B collocation points yields the following equations

$$\bar{u}(\mathbf{x}_i)=\sum_{l=1}^{N}\alpha_l\varphi_l(\mathbf{x}_i,\mathbf{x}_l)+\sum_{m=1}^{N_B}\beta_mG(\mathbf{x}_i,\mathbf{x}_m),\quad i=1,\cdots,N_I, \tag{3.2a}$$

https://doi.org/10.4208/aamm.2014.m611 Published online by Cambridge University Press

$$\bar{u}(\mathbf{x}_j)=\sum_{l=1}^{N}\alpha_l\varphi_l(\mathbf{x}_j,\mathbf{x}_l)+\sum_{m=1}^{N_B}\beta_m G(X_j,X_m), \qquad j=1,\cdots,N_B, \tag{3.2b}$$

$$\bar{q}(\mathbf{x}_k)=\sum_{l=1}^{N}\alpha_l\frac{\partial\varphi_l(\mathbf{x}_k,\mathbf{x}_l)}{\partial n}+\sum_{m=1}^{N_B}\beta_m\frac{\partial G(\mathbf{x}_k,\mathbf{x}_m)}{\partial n}, \qquad k=1,\cdots,N_B. \tag{3.2c}$$

Eqs. (3.2a)-(3.2c) can be written in the matrix form as

$$A\lambda=b, \tag{3.3}$$

where A and b are $(N+N_B)\times(N+N_B)$ known matrix and $(N+N_B)$ vectors, respectively.

After the coefficient is solved, we can approximate the unknown source function f with a finite series of basis functions

$$f(\cdot)=\sum_{l=1}^{N}\alpha_l\psi_l(\cdot), \tag{3.4}$$

where ψ_l must satisfy $\Delta\varphi_l=\psi_l$.

Note that if only part of the boundary $\partial\Omega$ is accessible, the system of linear algebraic equations (3.3) is ill-conditioned. Direct approaches, such as Gaussian elimination or the least-squares method, would produce unstable solutions due to the ill-conditioned coefficient matrix A. As the number of boundary points increases, the condition number of A increases dramatically. This problem can be cured by regularization techniques [16, 34,37]. In this paper, we use the Tikhonov regularization (TR) method, which is one of the most popular regularization methods, to solve the matrix system (3.3). The regularization procedure will be briefly described below.

3.2 Tikhonov regularization method

Using the singular value decomposition, we can decompose the matrix A in Eq. (3.3) as [2]

$$A=UDV^T, \tag{3.5}$$

where $U=[u_1,u_2,\cdots,u_{N+N_B}]$ and $V=[v_1,v_2,\cdots,v_{N+N_B}]$ are matrices with orthonormal columns, u_i and v_i are the left and right singular vectors of A, respectively. $U^TU=V^TV=I$ is the identity matrix, D is a diagonal matrix with diagonal entries $\sigma_1\geq\sigma_2\geq\cdots\geq\sigma_K>0$, where σ_i $(1\leq i\leq K)$ are the singular values of A.

We can seek for a stabilized solution for Eq. (3.3) by Eq. (3.5) in the following form

$$\lambda=\sum_{i=1}^{K}\frac{u_i^Tb}{\sigma_i}v_i. \tag{3.6}$$

The basic theory of the TR is to replace Eq. (3.3) with the minimization problem

$$\min_{\alpha\in\mathbb{R}^n}\|A\lambda-b\|^2+\mu^2\|\lambda\|^2. \tag{3.7}$$

https://doi.org/10.4208/aamm.2014.m611 Published online by Cambridge University Press

Here, $\mu \geq 0$ is a regularization parameter and $\|\cdot\|$ is the Euclidean norm. Its solution can be expressed as

$$\lambda_\mu = \lambda_{\min} = \sum_{i=1}^{K} \frac{\sigma_i u_i^T b}{\sigma_i^2 + \mu^2} v_i, \tag{3.8}$$

where the summation index upper-bound K is the rank of A. Readers are referred to [13, 16] for further details.

In order to obtain a good regularization parameter, we adopt the generalized cross validation (GCV) method which is a statistical method [16]. It estimates the optimal value of the regularization parameter by minimizing the functional

$$V_\mu = \frac{K\|A\lambda_\mu - b\|^2}{[\text{trace}(I - A_\mu)]^2}, \tag{3.9}$$

where A_μ is the influence matrix satisfying $A\lambda_\mu = A_\mu b$. After solving the TR equation (3.7) to determine the unknown coefficients λ, the unknown source distribution f can readily be calculated by Eq. (3.4).

4 Numerical experiments

Throughout the section, numerical results will be illustrated using the relative root mean-square error (RMSE) defined as [33]:

$$\text{RMSE} = \sqrt{\frac{1}{N_t} \sum_{j=1}^{N_t} (\text{Rerr})^2}, \tag{4.1}$$

where $\text{Rerr} = |u(\cdot) - \tilde{u}(\cdot)|/|u(\cdot)|$ for $|u(\cdot)| \geq 10^{-3}$ and $\text{Rerr} = |u(\cdot) - \tilde{u}(\cdot)|$ for $|u(\cdot)| > 10^{-3}$ with $u(\cdot)$ and $\overline{u}(\cdot)$ denote the analytical and numerical solutions, respectively. N_t is the total test point number. Not that MATLAB regularization code developed by Hansen [16] has been used in our computations.

Our first example studies the effects of MQ parameters on the accuracy of the proposed scheme. Next, we analyze the convergence curves of the RMSE versus the boundary point numbers. After that, the effect of different internal point numbers on the accuracy of the proposed method is discussed. Moreover, numerical performance is tested with various boundary noisy data whilst the other parameters of the method are kept fixed. The second example considers another case on an irregular domain. The last example examines the problem with the high frequency trigonometric source function.

4.1 Case 1: circular domain

For the unit circular domain $\Omega = \{(x,y)|x^2 + y^2 \leq 1\}$, we consider inverse source problem with the analytical solution $u(x,y) = x + \sin y$. The corresponding wavenumber and analytical source function are $\lambda = 1$ and $f(x,y) = x$, respectively.

https://doi.org/10.4208/aamm.2014.m611 Published online by Cambridge University Press

4.1.1 Influence of MQ shape parameters

It is well-known that the MQ solution accuracy is sensitive to the shape parameter. Some techniques have been proposed to determine the proper MQ shape parameter [11, 12, 17, 39]. Hence, we first consider the influence of the shape parameters on numerical solutions.

We fix the internal point number $N_I = 3$ for this case, this will soon be justified in Section 4.1.3. Fig. 1 provides the curve of numerical solutions versus different MQ shape parameters c, while the boundary point number $N_B = 10$ is fixed. Although there's a small oscillation when shape parameter $c \in (1,3)$, we find that the numerical solutions is becoming more and more accurate at a stable rate with increasing shape parameters. Unless otherwise stated, we choose $c = 10$ in the following cases.

4.1.2 Convergence curves of the RMSE

To investigate the stability of the proposed method, Fig. 2 displays the RMSE versus the boundary point number with fixed internal point number $N_I = 3$. The relative average error decreases until the boundary point number $N_B \leq 7$. After $N_B > 7$, a further increase in the boundary point numbers does not improve numerical results obviously at about RMSE$\approx 10^{-3}$. This reveals that even when using a relatively small boundary point

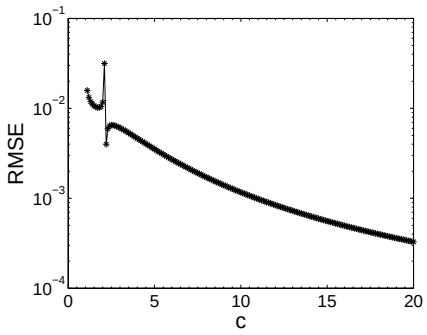


Figure 1: Shape parameters c versus RMSE.

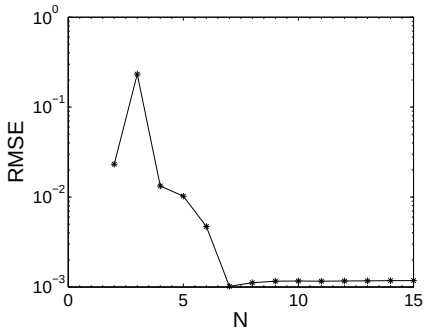


Figure 2: RMSE versus boundary point number N.

https://doi.org/10.4208/aamm.2014.m611 Published online by Cambridge University Press

numbers can yield accurate numerical results. So, we choose $N_B = 7$ in the following discussions.

4.1.3 Influence of internal point numbers

When using the dual reciprocity method to solve inhomogeneous problems, some internal points are always considered to improve solution accuracy. Another technique without any internal collocation point, called the multiple reciprocity method was developed by Nowak and his coworkers [26]. Indeed, the problem (2.1) we considered can also be solved by the multiple reciprocity method. But such a method encounters similar restrictions as in the scheme of [18], that is, the source function needs to satisfy definite governing equations. This issue is beyond the scope of our current research and thus will not be discussed here. In this paper, we also consider the effect of internal point numbers to solution accuracy of the proposed method.

Fig. 3 reveals the exact source distribution (Fig. 3(a) and numerical source distributions with internal point numbers $N_I = 0$ in Fig. 3(b), $N_I = 2$ in Fig. 3(c) and $N_I = 3$ in Fig. 3(d), respectively. We notice that the numerical results without internal point cannot reasonably simulate the source function. As two internal points are added, the proposed method can simulate the source function very well with RMSE $= 2.90 \times 10^{-3}$. After the internal point number increases to $N_I = 3$, the relative average error has the same order of accuracy with RMSE $= 1.02 \times 10^{-3}$. Although not presented here, we find internal

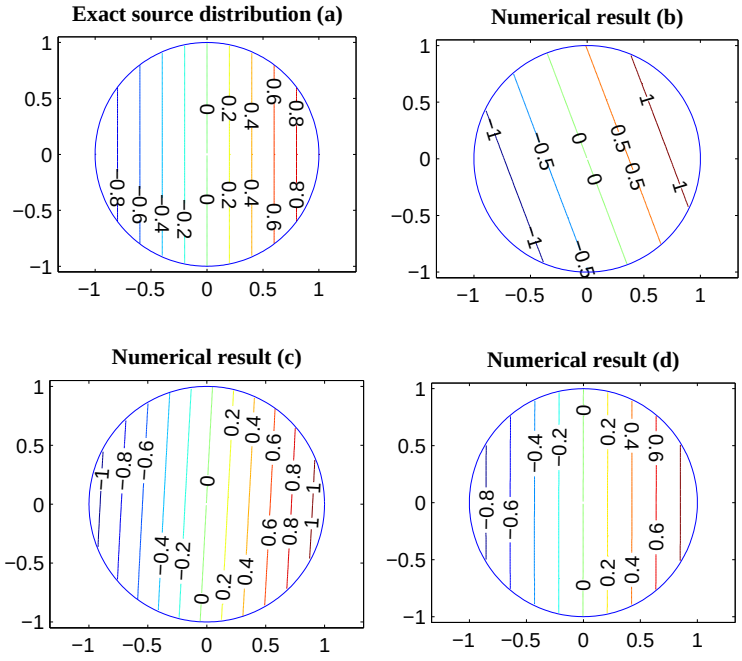


Figure 3: Source distributions for Section 4.1.3.

https://doi.org/10.4208/aamm.2014.m611 Published online by Cambridge University Press

point numbers $N_I \geq 3$ yield similar numerical results. Thus, we recommend using $N_I = 3$ internal point number for all cases.

4.1.4 Influence of accessible boundary data

Here, we consider the effect of accessible boundary

$$\Gamma = \{(r,\theta) | r = 1,\ 0 \leq \theta < \alpha\} \tag{4.2}$$

on the accuracy of the proposed method, where the polar angle $\alpha \in [\pi/4, 2\pi]$. Fig. 4 shows the sensitivity of numerical accuracy with respect to the measurement of the accessible boundary Γ with angle step $\pi/4$.

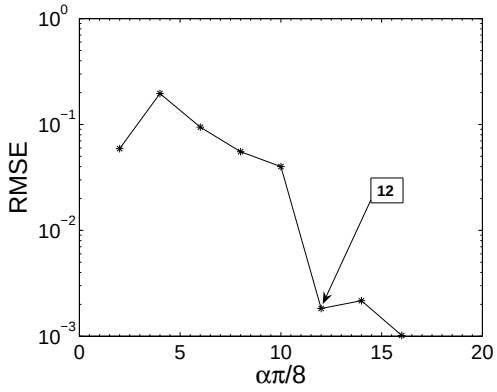


Figure 4: Numerical results obtained with the variation of accessible boundary data.

From Fig. 4, we observe that the variation of numerical accuracy coincide with the accessible boundary. More specifically, more accessible boundary data will give more accurate solutions. However, a further increase of the accessible boundary $\alpha \geq 3\pi/2$ does not improve substantially the solution accuracy. This phenomenon reveals that only partly accessible boundary can yield acceptable numerical results for the present method. It is promising in solving problems with partly accessible boundary.

4.1.5 Noisy boundary data

For practical applications, the boundary data may be disturbed by some noise. Here, we add random additive noise to the boundary conditions on partly accessible boundary $\Gamma = \{(r,\theta) | r = 1,\ 0 \leq \theta < 3\pi/2\}$ by

$$u = \bar{u} + \delta, \quad q = \bar{q} + \delta, \tag{4.3}$$

where $\delta = \varepsilon \times \text{Rand}$. We use the uniform MATLAB random number generator Rand to produce random numbers in $[-1,1]$. Here, ε denotes the additive noise level.

For boundary point number $N = 7$, Table 1 shows the numerical results versus different noise levels. Even though all runs in Table 1 have exactly the same condition number,

https://doi.org/10.4208/aamm.2014.m611 Published online by Cambridge University Press

Table 1: Effect of noise level for Section 4.1.5.

noise percentage (%)	Cond	RMSE	GCV-TR
0.0001	3.18×10^{7}	2.80×10^{-3}	2.50×10^{-3}
0.001	3.18×10^{7}	1.26×10^{-2}	2.10×10^{-3}
0.01	3.18×10^{7}	1.13×10^{-1}	2.21×10^{-2}
0.1	3.18×10^{7}	1.12×10^{0}	4.05×10^{-2}

completely different error behaviors are observed in cases with higher noise levels. This phenomenon can be illustrated by the so called effective condition number [7, 36]. As expected, with higher noise level added, the solution accuracy decreases. The solution accuracy is proportional to the noise level, i.e., one decimal increase of noise level corresponds with one decimal increase of solution accuracy.

On the other hand, Table 1 suggests that numerical solutions are acceptable for the small noise $\varepsilon=0.0001$. Once the noise $\varepsilon=0.001$ is added, numerical solutions are not that reliable. Thus, we adopt regularization methods instead of applying numerical methods directly under such cases. For the noise $\varepsilon=0.1$ is added, the TR regularization method can improve the solution accuracy with about two decimal precision.

Corresponding to Table 1, Fig. 5 shows the additive noise distribution for $\varepsilon=0.1$ and $\varepsilon=0.01$. From which we see that the boundary with noise level $\varepsilon=0.1$ is obviously different from the ideal one. The boundary with noise level $\varepsilon=0.01$ is similar with the ideal one. For smaller noise levels, the noise distribution is almost coincide with the ideal one. Thus, they are not shown in this figure.

Fig. 6 presents the GCV function $G(\lambda)$ obtained for the inverse source problem using the Tikhonov regularization method to solve the BKM system of Eqs. (3.3), and with various levels of noise ε. From this figure, it can be seen that the minimum of $G(\lambda)$ occurs approximately at $\lambda=12.55$ and $\lambda=5.671$ for $\varepsilon=0.1$ and $\varepsilon=0.01$, respectively. For both $\varepsilon=0.001$ and $\varepsilon=0.0001$, the corresponding λ are the same ($\lambda=3.53\times10^{-4}$) for the minimum of $G(\lambda)$. This reveals that there's no need to use regularization method for

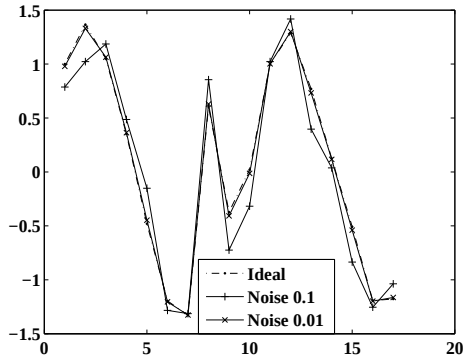


Figure 5: The additive noise distribution for $\varepsilon=0.1$ and $\varepsilon=0.01$.

https://doi.org/10.4208/aamm.2014.m611 Published online by Cambridge University Press

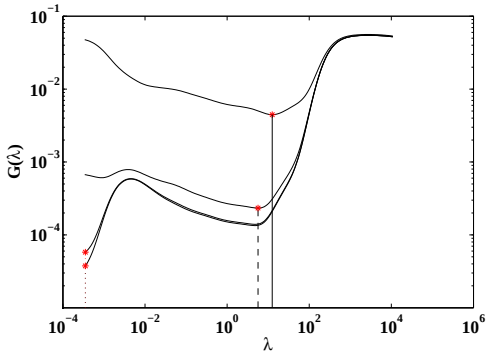


Figure 6: The corresponding generalized cross validation for $\varepsilon=0.1(-)$, $\varepsilon=0.01(--)$, $\varepsilon=0.01(\cdots)$ and $\varepsilon=0.01(\cdots)$.

smaller noise levels which coincide with the results shown in Table 1. Similar results have been obtained for the other problems investigated in this study and, therefore, they are not presented here.

4.2 Case 2: irregular domain

We reconsider the inverse source problem on an irregular domain, i.e., submarine cross section (Fig. 7). This time, the analytical source function is chosen to be $f(x,y)=2e^x$ with corresponding analytical solution $u(x,y)=e^x+\sin y$ and wavenumber $\lambda=1$.

Fig. 8 shows the relation between boundary point numbers and RMSE. While the MQ shape parameter $c=12.5$ is fixed, we note that the selection of MQ shape parameter is

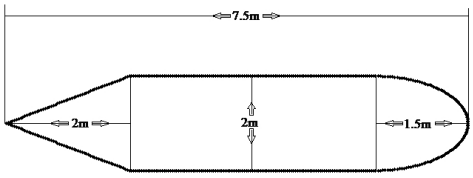


Figure 7: Submarine cross section.

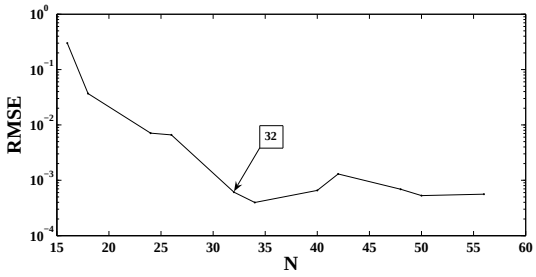


Figure 8: RMSE versus boundary point number N.

https://doi.org/10.4208/aamm.2014.m611 Published online by Cambridge University Press

the same as the previous example. We can see that convergence of the numerical solution accuracy is stable. Although there's a tiny oscillation when the boundary point number $N_B \geq 32$, the solution accuracy almost remains the same at about RMSE $= 10^{-3}$. We find that this results can compete with the previous case (Fig. 2). This phenomenon shows that the proposed method is irrelevant to the physical domain.

4.3 Case 3: trigonometric source function

The previous two cases considered problems with polynomial and exponential source functions. In fact, the method also works well for problems with trigonometric source functions. This problem will consider the problem with trigonometric source function $f(x,y) = \sin y$ under the unit circular domain $\Omega = \{(x,y)|x^2+y^2 \leq 1\}$. The corresponding analytical solution is $u(x,y) = \sin x \cos y + \sin y$ and wavenumber is $\lambda = 1$.

Fig. 9 shows the relation between boundary point numbers and RMSE. Under the way of choosing MQ shape parameter in Section 4.1.1, we fix the MQ shape parameter $c = 10$ in this example. We can see that convergence of the numerical solution accuracy is smooth for boundary point number $N_B \leq 6$. After the boundary point number $N_B \geq 6$, the solution accuracy almost remains the same at about RMSE $= 10^{-2}$. Even the numerical solution accuracy is enough reliable for engineering problems. We find that the RMSE results are larger than the previous two cases (Figs. 2 and 8). This phenomenon may contribute to the high frequency trigonometric smooth source function.

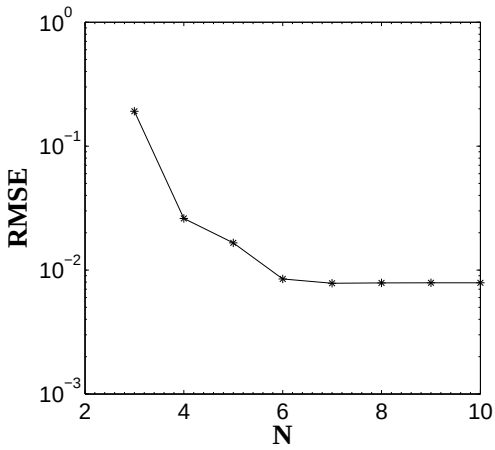


Figure 9: RMSE versus boundary point number N.

5 Conclusions

In this paper, a novel meshless scheme is proposed to deal with inverse source identification problems of Helmholtz-type equations. The present numerical procedure is based on

https://doi.org/10.4208/aamm.2014.m611 Published online by Cambridge University Press

the non-singular general solutions of the Helmholtz-type equations in conjunction with the radial basis functions. The Tikhonov regularization method under parameter of the generalized cross validation is employed for problems with noisy boundary data. Under this meshless scheme, we can determine the unknown source terms from partially accessible boundary measurements with accurate and stable numerical results. The proposed method can compete with the boundary-type meshless method since only a small number of internal points are needed during the whole process. However, our study focuses on the smooth unknown source function on the whole domain. A more systematic study on the non-smooth function deserves further investigation.

Acknowledgments

The author would like to thank the editor and referees for the helpful suggestions. The second author is supported by the Excellent Doctor Scientific Research Support Project of Jiangsu Normal University (No. 9212814103).

References

[1] C. J. S. Alves and R. R. S. Antunes, *The method of fundamental solutions applied to the calculation of eigensolutions for 2D plates,* Int. J. Numer. Methods Eng., 77 (2009), pp. 177–194.
[2] C. S. Chen, A. C. Hokwon and M. A. Golberg, *Some comments on the ill-conditioning of the method of fundamental solutions,* Eng. Anal. Boundary Elements, 30 (2006), pp. 405–410.
[3] C. S. Chen, S. W. Lee and C. S. Huang, *The method of particular solutions using Chebyshev polynomial based functions,* Int. J. Comput. Methods, 4 (2007), pp. 15–32.
[4] W. Chen and Y. C. Hon, *Numerical investigation on convergence of boundary knot method in the analysis of homogeneous Helmholtz, modified Helmholtz and convection-diffusion problems*, Comput. Methods Appl. Mech. Eng., 192 (2003), pp. 1859–1875.
[5] W. Chen and M. Tanaka, *A meshless, integration-free, and boundary-only RBF technique*, Comput. Math. Appl., 43 (2002), pp. 379–391.
[6] H. A. Cho, M. A. Golberg, A. S. Muleshkov and X. Li, *Trefftz methods for time dependent partial differential equations,* Comput. Materials Continua, 1 (2004), pp. 1–37.
[7] T. W. Drombosky, A. L. Meyer and L. Ling, *Applicability of the method of fundamental solutions*, Eng. Anal. Boundary Elements, 33 (2009), pp. 637–643.
[8] B. A. El, *Inverse source problem in an anisotropic medium by boundary measurements,* Inverse Problems, 21 (2005), pp. 1487–1506.
[9] G. Fairweather and A. Karageorghis, *The method of fundamental solutions for elliptic boundary value problems*, Adv. Comput. Math., 9(1-2) (1998), pp. 69–95.
[10] A. Farcas, *Dual reciprocity boundary element methods for solving inverse problems: applications to inverse source and boundary value problems for the poisson equation,* Saarbrucken: Lambert Academic Publishing, 2010.
[11] G. E. Fasshauer and J. G. Zhang, *On choosing "optimal" shape parameters for RBF approximation,* Numer. Algorithms, 45 (2007), pp. 345–368.
[12] B. Fornberg and G. Wright, *Stable compuatation of multiquadric interpolants for all values of the shape parameter,* Comput. Math. Appl., 48 (2004), pp. 853–867.

https://doi.org/10.4208/aamm.2014.m611 Published online by Cambridge University Press

[13] G. H. Golub, P. C. Hansen and D. P. O. Leary, *Tikhonov regularization and total least squares*, SIAM J. Matrix Anal. Appl., 21(1) (1999), pp. 185–194.
[14] Y. Gu, W. Chen and Z. J. Fu, *Singular boundary method for inverse heat conduction problems in general anisotropic media*, Inverse Problems Sci. Eng., 22 (2013), pp. 889–909.
[15] Y. Gu, W. Chen and X. Q. He, *Improved singular boundary method for elasticity problems*, Comput. Struct., 135 (2014), pp. 73–82.
[16] P. C. Hansen, *Regularization tools: A Matlab package for analysis and solution of discrete ill-posed problems*, Numer. Algorithms, 6 (1994), 1–35.
[17] C. S. Huang, C. F. Lee and A. H. D. Cheng, *Error estimate, optimal shape factor, and high precision computation of multiquadric collocation method*, Eng. Anal. Boundary Elements, 31 (2007), pp. 614–623.
[18] B. T. Jin and L. Marin, *The method of fundamental solutions for inverse source problems associated with the steady-state heat conduction*, Int. J. Numer. Methods Eng., 69 (2007), pp. 1570–1589.
[19] Y. Kagawa, Y. H. Sun and O. Matsumoto, *Inverse solution for Poisson equations using DRM boundary element models–identification of space charge distribution*, Inverse Problems Sci. Eng., 1 (1995), pp. 247–265.
[20] E. J. Kansa, *Multiquadrics-a scattered data approximation scheme with applications to computational fluid-dynamicsłI surface approximations and partial derivative estimates*, Comput. Math. Appl., 19(8-9) (1990), pp. 127–145.
[21] A. Karageorghis, D. Lesnic and L. Marin, *A survey of applications of the MFS to inverse problems*, Inverse Problems Sci. Eng., 19 (2011), pp. 309–336.
[22] E. Kita and N. Kamiya, *Trefftz method: an overview*, Adv. Eng. Software, 24(1-3) (1995), pp. 3–12.
[23] L. Ling, Y. C. Hon and M. Yamamoto, *Inverse source identification for Poisson equation*, Inverse Problems Sci. Eng., 13 (2005), pp. 433–447.
[24] F. Martinus, D. W. Herrin and D. J. Han, *Identification of an aeroacoustic source using the inverse boundary element method*, Noise Control Eng. J., 58 (2010), pp. 83–92.
[25] T. Nara and S. Ando, *A projective method for an inverse source problem of the Poisson equation*, Inverse Problems, 19 (2003), pp. 355–369.
[26] A. J. Nowak and A. C. Neves, The Multiple Reciprocity Boundary Element Method, Computational Mechanic Publications, Southampton, 1994.
[27] K. Ohnaka and K. Uosaki, *Boundary element approach for identification of point forces of distributed parameter systems*, Int. J. Control, 49 (1989), pp. 119–127.
[28] P. W. Partridge, C. A. Brebbia and L. W. Wrobel, The Dual Reciprocity Boundary Element Method, Computational Mechanic Publication, Southampton, 1992.
[29] A. Poullikkas, A. Karageorghis and G. Georgiou, *Method of fundamental solutions for harmonic and biharmonic boundary value problems*, Comput. Mech., 21 (1998), pp. 416–423.
[30] A. Schuhmacher, J. Hald, K. B. Rasmussen and P. C. Hansen, *Sound source reconstruction using inverse boundary element calculations*, J. Acoustical Soc. Amer., 1 (2003), pp. 114–127.
[31] M. Trlep, A. Hamler and B. Hribernik, *The use of DRM for inverse problems of Poisson's equation*, IEEE Trans. Magn., 36 (2000), pp. 1649–1652.
[32] F. Z. Wang, *Applicability of the boundary particle method*, Comput. Model. Eng. Sci., 80(3) (2011), pp. 201–217.
[33] F. Z. Wang, *Numerical simulation of acoustic problems with high wavenumbers*, Appl. Math. Inform. Sci., 9(2) (2015), pp. 1–4.
[34] F. Z. Wang, W. Chen and X. R. Jiang, *Investigation of regularized techniques for boundary*

https://doi.org/10.4208/aamm.2014.m611 Published online by Cambridge University Press

knot method, Int. J. Numer. Methods Biomedical Eng., 26(12) (2010), pp. 1868–1877.
[35] F. Z. WANG, W. CHEN AND L. LING, *Combinations of the method of fundamental solutions for general inverse source identification problems*, Appl. Math. Comput., 219(3) (2012), pp. 1173–1182.
[36] F. W. WANG, L. LING AND W. CHEN, *Effective condition number for boundary knot method*, Comput. Materials Continua, 12 (2009), pp. 57–70.
[37] T. WEI, Y. C. HON AND L. LING, *Method of fundamental solutions with regularization techniques for Cauchy problems of elliptic operators*, Eng. Anal. Boundary Elements, 31 (2007), pp. 373–385.
[38] P. H. WEN AND C. S. CHEN, *The method of particular solutions for solving scalar wave equations*, Int. J. Numer. Methods Eng., 26 (2010), pp. 1878–1889.
[39] J. WERTZ, E. J. KANSA AND L. LING, *The role of the multiquadric shape parameters in solving elliptic partial differential equations*, Comput. Math. Appl., 51 (2006), pp. 1335–1348.
[40] J. Y. ZHANG AND F. Z. WANG, *Boundary knot method: an overview and some novel approaches*, Comput. Model. Eng. Sci., 88(2) (2012), pp. 141–154.

https://doi.org/10.4208/aamm.2014.m611 Published online by Cambridge University Press